



# Glucose concentration control of a fed-batch mammalian cell bioprocess using a nonlinear model predictive controller



Stephen Craven<sup>a</sup>, Jessica Whelan<sup>a</sup>, Brian Glennon<sup>b,\*</sup>

<sup>a</sup> Applied Process Company (APC) Ltd, NovaUCD, Belfield Innovation Park, Dublin 4, Ireland

<sup>b</sup> School of Chemical & Bioprocess Engineering, University College Dublin, Belfield, Dublin 4, Ireland

## ARTICLE INFO

### Article history:

Received 28 February 2013

Received in revised form 10 February 2014

Accepted 11 February 2014

Available online 21 March 2014

### Keywords:

Simulation

Real-time implementation

Nonlinear model predictive control

Performance indices

Bioprocess model

## ABSTRACT

A non-linear model predictive controller (NMPC) was investigated as a route to delivering improved product quality, batch to batch reproducibility and significant cost reductions by providing a means for better controlling the bioreactor environment in a Chinese hamster ovary (CHO) mammalian cell fed-batch process.

A nonlinear fundamental bioprocess model was developed to represent the CHO mammalian cell fed-batch bioprocess under study. This developed nonlinear model aided in the configuration and tuning of a NMPC through off-line simulation. The tuned NMPC was applied to a 15 L pilot-plant bioreactor for glucose concentration fixed set-point control. Traditionally, bioprocesses are characterized by long critical process parameter (CPP) measurement intervals (24 h). However, advances in PAT have helped increase CPP measurement frequency. An in situ Kaiser RXN2 Raman spectroscopy instrument was used to monitor the glucose concentration at 6 min intervals.

Glucose concentration control of a bioreactor is not a trivial task due to high process variability, measurement noise and long measurement intervals. Nevertheless, NMPC proved successful in achieving closed loop fixed set-point control in the presence of these common bioprocess operation attributes.

© 2014 Elsevier Ltd. All rights reserved.

## 1. Introduction

The biopharmaceutical sector represents a significant and growing division of the general pharmaceutical industry. The number of biopharmaceuticals currently on the market is just in excess of 200 and in 2009, they generated \$99 billion in sales. The market is predicted to grow between 7 and 15% annually over the next several years and by 2013, four of the five top-selling drugs will be protein-based products [1].

The control of bioprocesses is in its infancy in comparison to the chemical and traditional pharmaceutical sectors. This is due in part to the challenges associated with bioreactor control: poor process understanding, the lack of measurement of relevant process parameters and difficulties inherent in controlling bioprocesses which are dynamic, complex and non-linear. Process control of bioreactors seeks to influence the complex intracellular reactions of billions of cells by controlling their extracellular environment [2].

Historically it has been observed that mammalian cell numbers and total protein productivity can be dramatically increased

with lowered process concentrations of the byproducts associated with mammalian cell metabolism. The main byproducts of mammalian cell metabolism are lactate and ammonia which result from glucose and glutamine consumption, respectively. Controlling the glucose and glutamine concentrations in a bioreactor to reduced levels forces a metabolic shift, which results in cells becoming much more efficient in their use of the available nutrients [3,4].

Current industrial control of nutrient levels is predominately manual. Bolus feeds are generally introduced at 24 h intervals based on off-line analysis of daily process samples and *a priori* process knowledge [5,6]. However, these feeding strategies are labor intensive involving sampling, recalculation, and manual adjustments.

To reduce batch variation and improve process economics, many biopharmaceutical manufacturers aim to move beyond today's "quality-by-inspection" methodology and adopting quality by design (QbD) methods under the FDA's process analytical technologies (PAT) initiative. These methods center on measuring critical quality attributes and critical process parameters during processing. Application of the latest sensor technologies such as mass and Raman spectroscopy enables cell characteristics as well as substrate and metabolic byproduct concentrations to be measured online or at-line in a bioreactor [7]. Timely availability of such data helps improve the operators' knowledge of the bioprocess and thus enhances model development and the creation of

\* Corresponding author. Tel.: +353 1 716 1954; fax: +353 1 716 1177.

E-mail addresses: [stephen.craven@aprocess.com](mailto:stephen.craven@aprocess.com) (S. Craven), [brian.glennon@ucd.ie](mailto:brian.glennon@ucd.ie) (B. Glennon).

## Nomenclature

$A$	ammonia concentration (mM)
$C_i$	inhibitor concentration (mM)
$C_i^*$	inhibitor saturation concentration (mM)
$d$	magnitude of process-model mismatch (mM)
$e$	error between process variable and set-point (mM)
$F$	feed-rate ( $L\ h^{-1}$ )
$G$	glucose concentration (mM)
$k$	sample interval (h)
$k_{d,Q}$	degree of degradation of glutamine ( $h^{-1}$ )
$K_L$	lactate saturation constant (mM)
$K_A$	ammonia saturation constant (mM)
$K_G$	glucose saturation constant (mM)
$K_Q$	glutamine saturation constant (mM)
$k_d$	death rate ( $h^{-1}$ )
$k_{d,max}$	maximum death rate ( $h^{-1}$ )
$k_\mu$	intrinsic death rate ( $h^{-1}$ )
$K_{LYSIS}$	rate of cell lysis ( $h^{-1}$ )
$L$	lactate concentration (mM)
$m_G$	glucose maintenance coefficient ( $mmol\ cell^{-1}\ h^{-1}$ )
$m_Q$	glutamine maintenance coefficient ( $mmol\ cell^{-1}\ h^{-1}$ )
$M$	control horizon
$P$	prediction horizon
$Q$	glutamine concentration (mM)
$q_i$	specific inhibitor production rate ( $h^{-1}$ )
$S_G$	glucose concentration in the feed (mM)
$S_Q$	glutamine concentration in the feed (mM)
$u$	control action ( $L\ h^{-1}$ )
$V$	volume (L)
$X_T$	total cell density ( $cells\ L^{-1}$ )
$X_D$	dead cell density ( $cells\ L^{-1}$ )
$X_V$	viable cell density ( $cells\ L^{-1}$ )
$y$	process variable (mM)
$y_{sp}$	set-point (mM)
$\hat{y}$	model predictions (mM)
$Y_{A,Q}$	yield of ammonia from glutamine
$Y_{L,G}$	yield of lactate from glucose
$Y_{X,G}$	yield of cells from glucose ( $cells\ mmol^{-1}$ )
$Y_{X,Q}$	yield of cells from glutamine ( $cells\ mmol^{-1}$ )
<b>Greek symbols</b>	
$\Gamma$	diagonal elements of output weight matrix
$\Lambda$	diagonal elements of input weight matrix
$\mu$	growth rate ( $h^{-1}$ )
$\mu_{max}$	maximum growth rate ( $h^{-1}$ )

more sophisticated automation and control systems used in such processes.

There are many academic projects focusing on following this trend through the application of automated open and closed loop nutrient concentration control strategies using predefined feeds and feeds determined using on-line or at-line sensors to measure the process variable (PV), respectively [8]. On-line models have also been used to estimate the nutrient concentration with an at-line sensor used to periodically update the model [6]. Lu et al. [8] demonstrated two different automated cell culture control strategies. The first method was based upon on-line capacitance measurements where cultures were fed based on an on-line calculation involving growth and nutrient consumption rates. The second method was based upon automated glucose measurements obtained from the Nova Bioprofile FLEX autosampler (Nova

Biomedical, UK) where cultures were fed to maintain a target glucose level by using an on-line feedback calculation.

Lee et al. [9] used a low-glutamine fed-batch feedback control-loop process in attempting to control ammonia and lactate for a 293-HEK mammalian cell bioprocess for adenovirus production. The control algorithm consisted of a simple on-line calculation. Controlling glutamine levels at 0.1 mM, with no other modifications improved cell density and gave a 10-fold improvement in virus titer. Li et al. [10] controlled glucose at 0.3 mM and glutamine at 0.5 mM via an online closed loop feeding calculation, which related to ammonia and lactate levels decreasing by 74% and 63%, respectively. Their cultures extended from eight to 14 days, with a 1.7-fold increase in monoclonal antibody (MAb) titers.

Bioprocesses are inherently nonlinear and are traditionally associated with long nutrient concentration measurement intervals. Furthermore in a PAT environment, where the nutrient concentration is determined online via a spectroscopic technique, measurement noise is prevalent. The aforementioned closed-loop control strategies, based on simple online calculations of the controller output may not be advantageous or optimal for the nutrient concentration control of bioprocesses portraying such attributes.

In this study, nutrient concentration control was accomplished through the application of a model predictive controller (MPC). Model predictive control, also referred to as receding horizon control and moving horizon optimal control, has been widely adopted in industry [11–15] and is currently the most widely used of all model-based advanced control methodologies for industrial applications. Qin and Badgwell [16] presented a survey of industrial model predictive control technology. Originally developed to meet the needs of power plants and petroleum refineries, MPC technology can now be found in a wide range of application areas, including chemicals, food processing, automotive, and aerospace applications [16]. Bioprocess applications of MPC have appeared in a number of academic projects recently. Aehle et al. [17] experimentally applied a MPC to indirectly control the oxygen mass consumed by mammalian cells in a bioreactor by manipulating the glutamine feed-rate. Ashoori et al. [18] simulated the use of MPC based on a detailed model for penicillin production in a fed-batch bioreactor. The main control goal was to get a pure product with a high concentration, by regulating temperature and pH at certain levels.

The name MPC stems from the idea of employing a model of the process to be controlled which is used to predict the future behavior. This prediction capability allows optimal control problems to be solved on-line, where tracking error, namely the difference between the predicted output and the desired reference, is minimized over a future horizon, possibly subject to constraints on the manipulated inputs and outputs. While linear model predictive control (LMPC) has been popular since the 1970s, the 1990s witnessed an increased interest from control theoretists as well as control practitioners in the area of nonlinear model predictive control (NMPC) [19,20] due to the need to operate processes under tighter performance specifications. At the same time, more constraints, stemming, for example, from environmental and safety considerations need to be satisfied. Often these demands can only be met when process nonlinearities and constraints are explicitly considered in the controller. In addition, if the system is highly nonlinear, such as bioprocesses, control based on the prediction from a linear model may result in unacceptable response [21]. In some cases, remarkable static errors exist, and in other cases, oscillation or even instability may occur [22]. Therefore, non-linear models should be used to describe the behavior of a highly non-linear bioprocess system. Nagy [23] applied NMPC to adequately control the nonlinear nature of a bioreactor process.

There are a number of difficulties associated with implementing a NMPC [24–28]. One of the major difficulties is the

identification of a suitable nonlinear model. Nonlinear models can be developed in various forms. Empirical approaches range from high-order polynomials and neural networks to piecewise linear models. Mechanistic models are also available from engineering first principles such as mass balances and rate equations. Nonlinear data-based empirical models require much more data and computational effort to train than linear models. Developing data-based models also requires cooperation with the operating plant to perform tests with enough excitation to reveal the dynamics of the systems of interest at each operating point. Such cooperation may not be forthcoming if the plant is already operational, as testing may interfere with daily operations to the detriment of product quality. The inevitable downtime which testing involves may also prove excessively costly to plant operations. Nevertheless, most of the non-linear MPC strategies have been based on the use of data-based nonlinear neural network models [29]. However, Qin and Badgwell [12] stated that due to the difficulty in data-based modeling of nonlinear processes, first principles models will become necessary in practice.

NMPC has unique traits that are not seen with LMPC. In the case of LMPC, the solution of the optimal control problem can be cast as the solution of a convex (quadratic) program and can be solved easily on-line at each sample time. Due to the nonlinear model, the NMPC calculation usually involves a non-convex, nonlinear optimization problem, for which the numerical solution is very challenging and computationally expensive. This is one of the many reasons why LMPC is more dominant than NMPC in industry.

The non-convexity of the NMPC optimization problem can be problematic and result in multiple local minima or maxima which are not optimal. This phenomenon is unique to NMPC and can lead to undesirable controller performance. Performance degradation due to the presence of non-globally optimal local minima can be avoided by providing good initial state estimates to the optimizer and appropriate constraints [30]. Additional steps can also be taken to prevent convergence to an undesired local solution such as shortening the prediction horizon. Tenny et al. [30] showed that unwanted local minima can be removed by this method.

The aforementioned complexities, which increase the computational load of the NMPC optimization, may lead to failure to converge to a solution within the specified sampling interval. Typical industrial sampling intervals in the refining and chemical sector are approximately 1 min. However, in the biopharmaceutical sector, sampling intervals in the order of hours would be acceptable due to the slow process dynamics. In an ideal NMPC, it is assumed that the feedback is available instantaneously at every sampling interval. However, the real-time implementation of NMPC is computationally intensive and a computational lag usually exists [30]. The control horizon has an important role to play in the computational burden. The larger the control horizon, the greater the computational load. Nagy et al. [31] showed that the CPU time only increases “linearly” with the control horizon length. Overall, the computational complexity associated with the real-time application of NMPC depends on the optimization strategy, the control horizon length and the process model chosen. In summary, NMPC presents unique problems that must be addressed to guarantee the validity of its application.

Advanced NMPC control strategies are relatively non-existent in the bioprocess industry, possibly due to the difficulty in building nonlinear bioprocess models and also the batch nature of their processes. Firstly, a simulation study was undertaken in the presence of an applicable nonlinear bioprocess model to illustrate the known advantages of advanced NMPC in a real environment with measurement noise and disturbances. Based on the simulation results, it was decided to apply an NMPC strategy to two different case

studies for real-time control of the glucose concentration in a 15 L bioreactor to a defined set-point of 11 mM. The first case study mimicked the classical non-PAT enabled environment where the nutrient concentration is measured offline or at-line over long measurement intervals. Finally, in the second case study an NMPC was developed and implemented to allow for the closed loop feedback control of the bioreactor glucose concentration in the presence of process-model mismatch resulting from bioprocess variability and measurement noise which is inherent with on-line spectroscopic techniques.

## 2. Materials and methods

### 2.1. Bioprocess operation

Experiments were conducted on a 15 L pilot scale bioreactor (Applikon Biotechnology, Ltd., Netherlands). The cell line used in this study was a suspension-adapted CHO 320 cell line bearing the recombinant interferon gamma (IFN- $\gamma$ ) gene, which was sourced from the Animal Cell Culture Technology Group (ACTG), University College Dublin (UCD), Ireland. The cells were grown in glucose-free Ex-Cell serum-free medium (Sigma-Aldrich) which was supplemented with glutamine and glucose to 4 mM and 20 mM, respectively. Pluronic F68 (0.1%, v/v), 1  $\mu$ M methotrexate (MTX), antifoam C (5 ppm) and 10 mL/L of penicillin–streptomycin were also added.

The pH, dissolved oxygen (DO), temperature and agitation were controlled at constant values of 7.2, 50% of air saturation, 37 °C and 120 rpm, respectively. 1 M NaOH and CO<sub>2</sub> gas were used to control pH. DO was controlled using air and oxygen supplied via a sparger. The oxygenation level in the bioreactor determined the supply of air and oxygen for DO control. Initially, the air flow-rate was increased to bring the DO to its required set-point of 50%. Once the air flow-rate reached its maximum value, oxygen was utilized as a controller output for DO control. The substrates (glucose and glutamine) and by-products (lactate and ammonia) were measured online with Raman spectroscopy using a Kaiser RXN2 system (Kaiser Optical Systems, Inc., USA) and off-line using the Nova Bio-profile 400 (Nova Biomedical, UK) [32]. Samples were taken daily at a minimum and the cell density and viability were measured using the trypan blue dye exclusion method. The bioreactor was run in fed-batch mode and fed continuously, the rate of which was determined and adjusted automatically using a nonlinear model predictive controller (NMPC) and Raman-based glucose measurements to keep the glucose concentration in the bioreactor at a set-point of 11 mM throughout the culture. The feed consisted of a combined mixture of glucose (653 mM), glutamine (58.8 mM) and soy hydrolysate powder (58.8 g/L) (Irvine Scientific, USA) dissolved in glucose-free Ex-Cell serum-free medium.

### 2.2. Bioprocess model

The bioprocess model was a nonlinear, first principle, mechanistic mathematical model which described the cell growth and the cell metabolism. It was based on certain standard assumptions, such as a well-mixed bioreactor and perfect control of culture pH, temperature and dissolved oxygen concentration.

The model consisted of eight first-order ordinary differential equations (Eqs. (1)–(8)) representing the rate of change of state variables of the process. The state variables included the total cell density ( $X_T$ ), viable cell density ( $X_V$ ), dead cell density ( $X_D$ ), glucose concentration ( $G$ ), glutamine concentration ( $Q$ ), lactate concentration ( $L$ ), ammonia concentration ( $A$ ) and an unknown inhibitor concentration ( $C_i$ ).  $S_G$  and  $S_Q$  were the concentrations of glucose and glutamine in the feed,  $F$ , respectively. The eight state variables were

**Table 1**  
Model parameters.

Parameter	Unit	Value
$k_{d,Q}^a$	$\text{h}^{-1}$	0.001
$m_G^a$	$\text{mmol cell}^{-1} \text{h}^{-1}$	$1.4 \times 10^{-10}$
$Y_{A,Q}^b$	–	0.90
$Y_{L,G}^b$	–	2.0
$Y_{X,G}^b$	$\text{cells mmol}^{-1}$	$1.70 \times 10^8$
$Y_{X,Q}^b$	$\text{cells mmol}^{-1}$	$1.3 \times 10^9$
$K_L^a$	mM	150
$K_A^a$	mM	40
$k_{d,\max}^b$	$\text{h}^{-1}$	0.01
$\mu_{\max}^b$	$\text{h}^{-1}$	0.048
$K_G^a$	mM	1.0
$K_Q^a$	mM	0.22
$m_Q^a$	$\text{mmol cell}^{-1} \text{h}^{-1}$	$7.0 \times 10^{-12}$
$k(\mu^a)$	$\text{h}^{-1}$	0.01
$K_{\text{LYSIS}}^a$	$\text{h}^{-1}$	0
$C_i^a$	mM	100
$q_i^a$	$\text{mmol cell}^{-1} \text{h}^{-1}$	$3.5 \times 10^{-10}$

<sup>a</sup> Fitted model parameter.<sup>b</sup> Experimentally determined model parameter

dependent on the growth ( $\mu$ ) and death rate ( $k_d$ ) of the bioprocess mammalian cell line (Eqs. (9) and (10)):

$$\frac{dX_T}{dt} = \mu X_V - K_{\text{LYSIS}} X_D - X_T \left( \frac{F}{V} \right) \quad (1)$$

$$\frac{dX_V}{dt} = (\mu - k_d) X_V - X_V \left( \frac{F}{V} \right) \quad (2)$$

$$\frac{dX_D}{dt} = k_d X_V - K_{\text{LYSIS}} X_D - X_D \left( \frac{F}{V} \right) \quad (3)$$

$$\frac{dG}{dt} = \left( \frac{F}{V} \right) (S_G - G) + \left( -\frac{\mu}{Y_{X/G}} - m_G \right) X_V \quad (4)$$

$$\frac{dQ}{dt} = \left( \frac{F}{V} \right) (S_Q - Q) + \left( -\frac{\mu}{Y_{X/Q}} - m_Q \right) X_V - k_{d,Q} Q \quad (5)$$

$$\frac{dL}{dt} = -Y_{L/G} \left( -\frac{\mu}{Y_{X/G}} - m_G \right) X_V - \left( \frac{F}{V} \right) L \quad (6)$$

$$\frac{dA}{dt} = -Y_{A/Q} \left( -\frac{\mu}{Y_{X/Q}} - m_Q \right) X_V + k_{d,Q} Q - \left( \frac{F}{V} \right) A \quad (7)$$

$$\frac{dC_i}{dt} = q_i X_V - \left( \frac{F}{V} \right) C_i \quad (8)$$

$$\mu = \frac{\mu_{\max}(G)(Q)(C_i^* - C_i)}{C_i^*(K_G + G)(K_Q + Q)((L/K_L) + 1)((A/K_A) + 1)} \quad (9)$$

$$k_d = k_{d,\max} \left( \frac{k_\mu}{\mu + k_\mu} \right) \quad (10)$$

The model parameters were determined either experimentally or fitted using the differential evolution (DE) technique [33] with constraints set based on a literature survey. Table 1 presents the model parameter values for this system. This nonlinear model was built to represent the growth and metabolism of the CHO mammalian cell fed-batch bioprocess for which nonlinearity is inherent. Full details of this first principle engineering model (Monod-type kinetics) and its associated parameter estimation are described in [34]. This model was used within the process simulator and within the NMPC framework.

### 2.3. NMPC development

The NMPC strategies were configured in the MATLAB 7.11.0 (R2010b) environment. The NMPC configuration was coded without the use of the MATLAB MPC toolbox. A block diagram for the NMPC implementation is shown in Fig. 1. The NMPC was used to control the glucose bioreactor concentration using a nonlinear dynamic model of the bioprocess (Eqs. (1)–(8)). The nonlinear model had the following form:

$$\dot{x} = f(x, u) \quad y = g(x) \quad (11)$$

where  $x$  is a vector of states,  $u$  is the vector of manipulated inputs and  $y$  is a vector of outputs. Integration of the model from time step  $k-1$  to current time step  $k$  is represented by:

$$\hat{x}_k = F_{t_s}(\hat{x}_{k-1}, u_{k-1}) \quad \hat{y}_{k/k-1} = g(\hat{x}_k) \quad (12)$$

where  $t_s$  is the sample time; the  $k:k-1$  subscript notation is used to indicate the prediction at step  $k$  based on measurements at step  $k-1$ . At step  $k$ , an output measurement is available:

$$y_k$$

and the model error is calculated:

$$d_k = y_k - \hat{y}_{k/k-1} \quad (13)$$

A hypothetical set of current and future control moves:

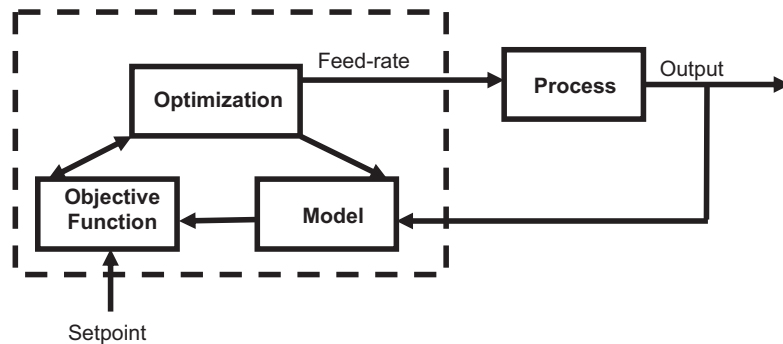
$$u_k, u_{k+1}, \dots, u_{k+P-1}$$

is chosen to minimize an objective function (Eq. (15)) over a prediction horizon of  $P$  steps, and the model is integrated from time step  $k$  to  $k+P$ , based on the hypothetical control moves

$$\hat{x}_{k+1} = F_{t_s}(\hat{x}_k, u_k) \quad \hat{y}_{k+1/k} = g(\hat{x}_{k+1}) + d_k \quad (14)$$

The objective function (Eq. (15)) was evaluated and the selection of control moves repeated until the optimum is obtained.

Note that the equations above assume that the plant-model mismatch was performed using the standard additive output disturbance assumption, similar to what is commonly assumed in

**Fig. 1.** Model predictive controller (MPC) architecture.



dynamic matrix control (DMC) [35].

$$\min_{\Delta u(t_k), \dots, \Delta u(t_{k+M-1})} \sum_{i=1}^P \left\| \Gamma(\hat{y}(t_{k+i}) - y_{sp}(t_{k+i})) \right\|^2 + \sum_{i=1}^M \left\| \Lambda \Delta u(t_{k+i-1}) \right\|^2 \quad (15)$$

There are many ways to integrate or solve the modeling equations and the optimization problem. Since its popularization in the late 1970s, sequential quadratic programming (SQP) has arguably become the most successful method for solving nonlinearly constrained optimization problems [36]. The most straightforward NMPC configuration is to use the SQP optimization strategy [37] as the “outer-loop” and a numerical model integrator as the “inner-loop” to evaluate the objective function (Eq. (15)) at each iteration of the optimizer. This technique known as the sequential (single shooting) strategy was utilized for the NMPC configurations, where the two steps, model integration and optimization, are performed sequentially, one after the other. This method of solution was chosen over the alternative simultaneous (multiple shooting) method due to the small-scale nature of the problem (8 ODEs) and the ease of construction associated with the sequential method. The simultaneous method of solution solves the two steps simultaneously within one loop at each optimization iteration. In the case of large scale problems, the simultaneous solution method would be more appropriate to deal with the computational intensities associated with the sequential method of solution were repeated numerical integration of the model ODEs is required [38].

The objective function (Eq. (15)) contains the NMPC tuning parameters: diagonal elements of output penalty weight matrix ( $\Gamma$ ), diagonal elements of input penalty weight matrix ( $\Lambda$ ), control horizon ( $M$ ) and prediction horizon ( $P$ ).  $y_{sp}$  is a vector of the predefined set-point trajectory,  $\hat{y}$  is a vector of model predictions over the prediction horizon,  $P$ , and  $\Delta u(t_k) = [\Delta u(t_k) \dots \Delta u(t_{k+M-1})]^T$  is a vector of  $M$  future changes of the control action vector  $u$  to be determined by the on-line optimization routine over a prediction horizon of length  $P$ . Only the current value of  $\Delta u$ , which is the first element of  $\Delta u(t_k)$ , is implemented on the plant, then at the next sampling time,  $k+1$ , the whole procedure is repeated. The penalty weighting matrices,  $\Gamma$  and  $\Lambda$  are used to trade off set-point tracking and manipulated variable movement, respectively.

Finally, the above objective function was minimized subject to the following constraints on the manipulated variable:

$$\Delta u_{\min} \leq \Delta u \leq \Delta u_{\max}$$

No constraints were applied to the PV in this study.

#### 2.4. NMPC performance simulation and real time application

Before an NMPC was applied in real time to the bioprocesses, offline simulations were conducted to optimally configure and tune the controller. MATLAB 7.11.0 (R2010b) was used as the offline simulation tool.

The fully tuned NMPC algorithm was applied online to the 15 L bioreactor. The nutrient and metabolite concentrations of the bioreactor system under study were monitored with an in-situ Kaiser RXN2 Raman spectroscopy probe which communicated via USB to the lab computer (Microsoft windows XP professional, Version 2002, Dell Optiplex 780, Intel® Core™2 Duo CPU, E7500 @ 2.93 GHz) containing the spectral acquisition software (iC Raman ver.4.1.910). Measurements were taken at 6 min intervals and the iC Raman software sent the collected spectral files to a specified file directory on the lab computer. In order to translate the spectral

data to nutrient and metabolite concentration values, a partial least squares (PLS) calibration model was built using the Eigenvector PLS toolbox (version 6.0.1) in MATLAB. This PLS calibration model was combined with the MATLAB coded NMPC algorithm and compiled into a single executable file using MATLAB Compiler (version 4.14). The MATLAB coded NMPC was applied to keep the glucose concentration in the bioreactor at a set-point by adjusting the feed-rate to the bioreactor. Fig. 2 graphically presents the method of controller deployment for the bioreactor system studied.

The PLS model/NMPC executable file was deployed on the lab computer. A shared network drive was created between the lab computer with the iC Raman software and the ABB 800xa DCS server (Microsoft windows server 2003, Intel® Xeon® CPU, E5520 @ 2.27 GHz). Based on the NMPC results sent by OPC, the ABB 800xa DCS communicated via an RS232 connection with a peristaltic pump to adjust the feed-rate accordingly.

#### 2.5. Controller performance indices

The performance of each simulated and real controller was quantified by calculating three different control measures: integral squared error (ISE), integral absolute error (IAE) and integral of the time multiplied by the absolute error (ITAE). They are defined by Eqs. (16)–(18), where  $e(t)$  is the error between the process variable and the defined set-point.

$$ISE := \int_0^t e(t)^2 dt \quad (16)$$

$$IAE := \int_0^t |e(t)| dt \quad (17)$$

$$ITAE := \int_0^t t |e(t)| dt \quad (18)$$

The ISE performance index integrates the squared error over time and is more sensitive to large deviations from the set-point. The IAE index integrates the absolute error over time and does not place weight on any of the errors in a system response. Finally, the ITAE index integrates the absolute error multiplied by time over time and penalizes errors that persist for a long period of time.

The three control measures are very precise and give exact comparisons between different control schemes. They are also among the most used controller performance indices.

### 3. Results and discussion

#### 3.1. Simulation study

A bioreactor is an integral component of a biopharmaceutical plant and the substrate concentration in the bioreactor is a critical process parameter that can be used to optimize the performance of the bioprocess. Therefore, it is a desirable target for control.

The behavior and performance of a control strategy can be simulated faster than real-time execution before on-line application. This is beneficial as bioprocesses have slow dynamics with a typical mammalian cell culture fed-batch process taking from 1 to 3 weeks and a perfusion process up to 3 months. Through simulation, one can also reduce the risk of control failures due to configuration errors and most importantly, save time without disturbing the process. Many different what-if scenarios can be tested in simulation mode. White Gaussian noise can be applied to the process variable (PV) as well as disturbances and their effect on performance analyzed. Simulation studies can also be used to help in developing a realistic process model which in turn can be used to help determine optimum operation conditions.

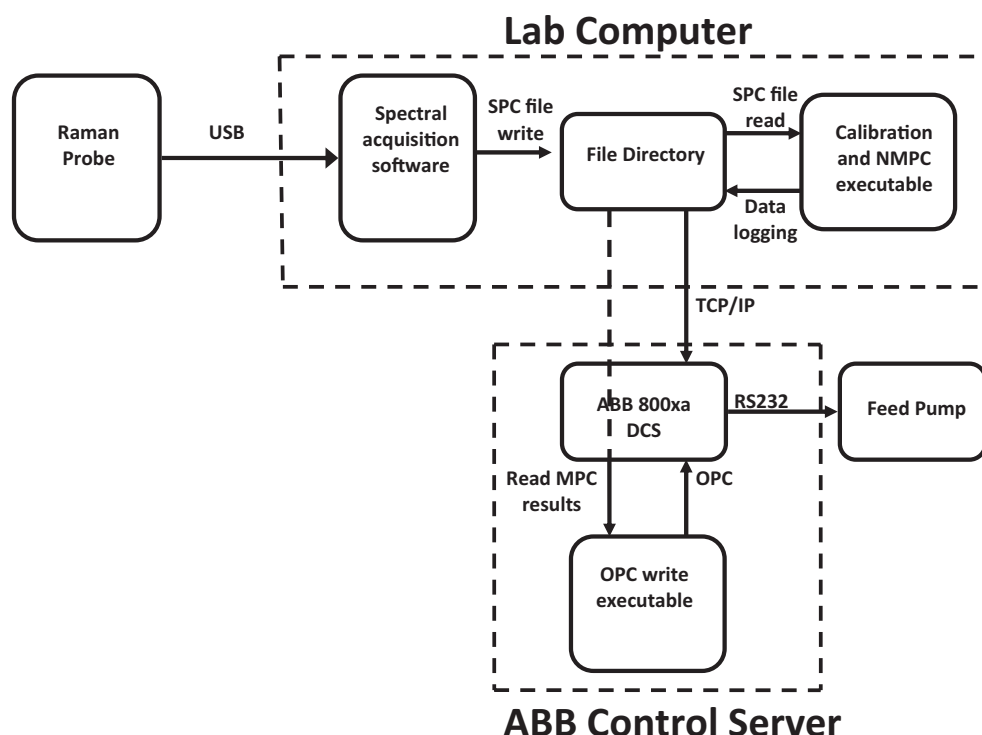


Fig. 2. Online NMPC deployment on 15 L pilot scale bioreactor schematic.

Measurement noise is a problem in most control loops. Noise gives false or erroneous process information which may result in unwarranted controller action. In bioprocesses the use of on-line spectroscopic techniques for nutrient and metabolite concentration determination is growing in popularity [32]. Such spectroscopic techniques have typically low signal to noise ratios (SNR). External filters on the controller output (CO) can be applied to help dampen out extreme chattering before the final control element (FCE) and thus avoid excessive wear and tear in the presence of measurement noise.

The performance of the single input–single output (SISO) NMPC was simulated based on a nonlinear, first principle, mechanistic mathematical model (Eqs. (1)–(8)) which described the cell growth and the cell metabolism for a CHO 320 cell line cultivated in a 15 L pilot scale fed-batch bioprocess [34]. The glucose concentration was chosen as the process variable for the bioprocess in this simulation study and was to be kept at a set-point of 11 mM until a planned step change to 15 mM was introduced at 100 h. This was accomplished by adjusting the feed-rate (CO) to the bioreactor. The sampling time was 0.1 h, which is acceptable for practical use. In the simulator, the bioprocess was associated with random (white) measurement noise with a signal to noise ratio (SNR) of 25 to approximate the noise associated with the Raman measurements.

Plant-model mismatch was avoided by utilizing the same model within the NMPC controller and process simulator. A long prediction horizon ( $P$ ) was used to ensure stability of the system and a small value for the control horizon ( $M$ ) was employed to reduce the online computational requirements. The diagonal elements of the output weight matrix,  $\Gamma$ , were set at 1 due to the single input–single output (SISO) nature of the process to be controlled. Finally, the diagonal elements of the input weight matrix,  $\Lambda$ , were increased from zero to make the response slower, more stable and help smooth the control action in the presence of measurement noise. At a zero value for  $\Lambda$ , the response was most aggressive. It was necessary to balance sluggish behavior and excessive

overshoot with noise rejection. The following NMPC tuning parameters were initially used:  $P = 10$ ,  $M = 1$ ,  $\Gamma = 1$ ,  $\Lambda = 0$ . Input magnitude constraints of  $0 \text{ L h}^{-1} \leq u \leq 4.07 \times 10^{-2} \text{ L h}^{-1}$  were imposed on the feed rate ( $u$ ). No constraints were set on the process variable ( $y$ ) as it may destabilize the feedback response [39].

The NMPC ( $P = 10$ ,  $M = 1$ ,  $\Gamma = 1$ ,  $\Lambda = 0$ ) control action in Fig. 3b reacted with chatter in the CO. However, NMPC has the huge benefit in that it has the potential to smooth out the control action. This can be done by adjusting the prediction horizon,  $P$ , and the diagonal elements of the input weight matrix,  $\Lambda$ . The prediction horizon,  $P$ , was re-tuned in the presence of measurement noise and increased until it has no further affect on the controller performance. The diagonal elements of the input weight matrix,  $\Lambda$ , was also increased to help dampen out the excessive controller output chattering that was observed when  $\Lambda = 0$ . This has to be balanced against the onset of sluggish control behavior as  $\Lambda$  increases [2]. Such NMPC tuning strategies are based on established rules of thumb and experience.

In a first attempt to improve the controller performance, the prediction horizon,  $P$ , was increased from 10 to 40. This allowed the model to look further into the future and thus improve the CO trajectory (Fig. 3d). The increased prediction horizon,  $P$ , resulted in an improved CO trajectory and dampened the chattering. The NMPC controller could foresee 4 h into the future and this reduced the effect of noisy measurement signals. However, the control action still exhibited some chattering in the presence of measurement noise. The next step was to increase the diagonal elements of the input weight matrix,  $\Lambda$ , to help further dampen the control action (Fig. 3f).

Increasing the diagonal elements of the input weight matrix,  $\Lambda$ , from 0 to 50000 reduced the CO chattering at the price of increased controller sluggishness. The ability to smoothen out the controller action in the presence of measurement noise is a beneficial quality for a controller within a mammalian cell bioprocess aiding in a reduction in the bioprocess batch to batch variation and the wear and tear of the FCE. However, a balance must be struck between an

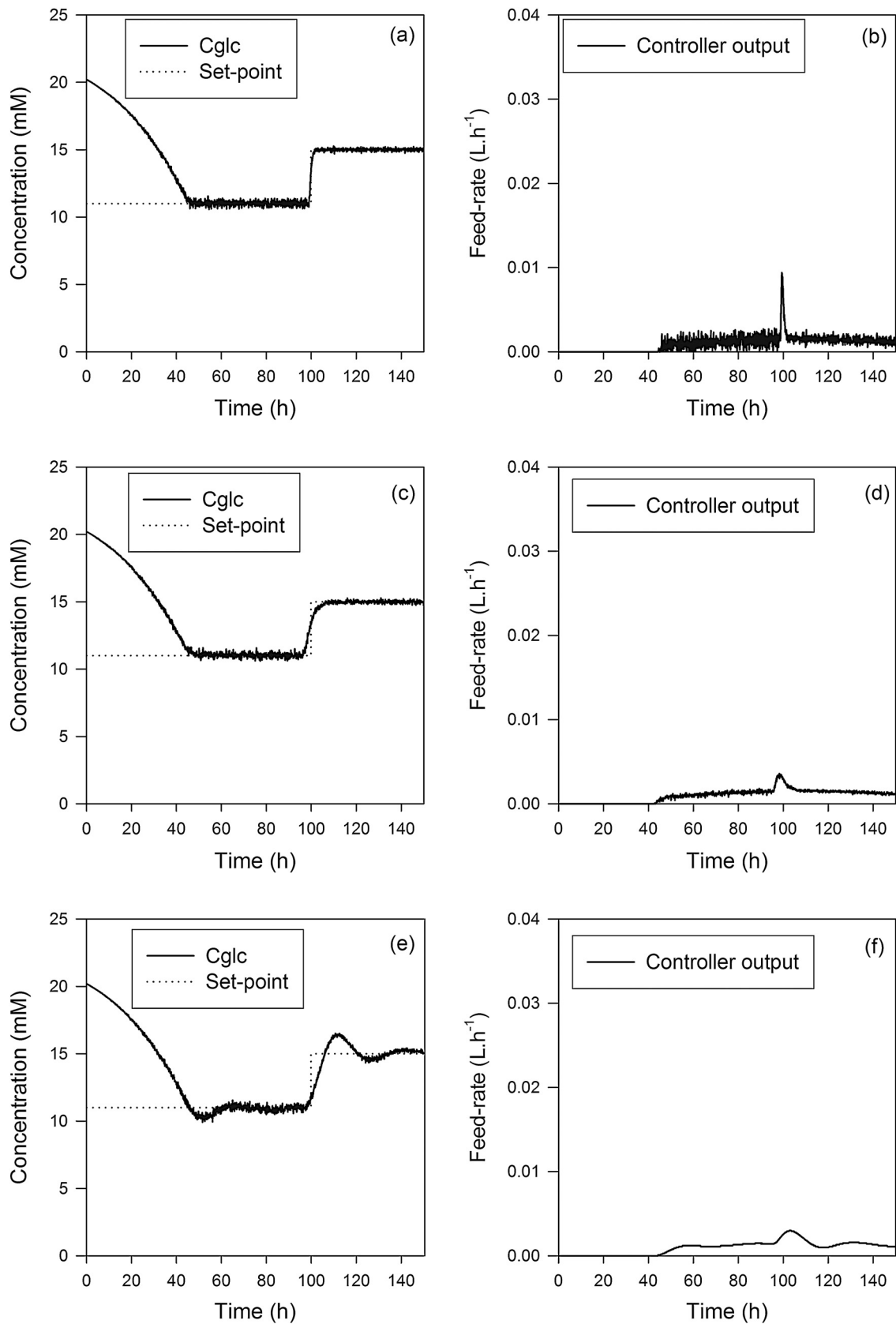


**Fig. 3.** Simulated NMPC set-point tracking performance for glucose in the presence of measurement noise and the corresponding controller output (a, b:  $P=10, M=1, \Gamma=1, \Lambda=0$ ; c, d:  $P=40, M=1, \Gamma=1, \Lambda=0$ ; e, f:  $P=40, M=1, \Gamma=1, \Lambda=50,000$ ).

**Table 2**  
Simulated NMPC performance indices for a 0.1 h measurement interval.

Index	NMPC ( $P=10, M=1, \Gamma=1, \Lambda=0$ )	NMPC ( $P=40, M=1, \Gamma=1, \Lambda=0$ )	NMPC ( $P=40, M=1, \Gamma=1, \Lambda=50,000$ )
ISE	17,303	17,372	17,709
ITAE	54,100	58,959	84,892
IAE	2665	2715	2968

increase in controller sluggishness and a reduction in CO chattering when tuning the NMPC for optimum controller performance [40]. The simulated NMPC performances were quantified using three different indices of performance (Table 2). The NMPC ( $P=10, M=1, \Gamma=1, \Lambda=0$ ) illustrated its optimality in set-point tracking which resulted in the lowest controller performance indices (ISE=17303, IAE=54100, ITAE=2665). However, more chatter was observed in its generated CO. In an attempt to dampen out this observed chatter in the control action, sluggishness was introduced to the system response (Fig. 3c and e) which resulted in higher performance indices (Table 2) based on an increase in the error between the process variable and the set-point.

### 3.2. Real-time NMPC glucose concentration control

In the bioprocessing industry, large sample times are common due to the unavailability of on-line PAT techniques for real time monitoring. Off-line instruments such as the Nova-Bioprofile 400 would be more prevalent in an industrial setting for supernatant composition monitoring than an on-line spectroscopic technique due to the workload and expertise associated with building a PLS calibration model for spectral analysis.

Due to the slow nature of bioprocess dynamics, traditional lack of on-line PAT instruments and an attempt to test the benefits of the NMPC prediction capabilities in a bioprocess environment, a NMPC sample time of 12 h was used. The Raman spectra were still collected at 6 min intervals, however, the NMPC would only operate at each 12 h interval in an attempt to mimic the industrial standard, a bioprocess without the availability of an on-line PAT instrument. The greater the NMPC sample time the more dependent the NMPC performance is on the applicability of the model to the process being controlled. Therefore every effort should be taken to ensure process-model mismatch is minimized.

The NMPC performance was simulated before real-time deployment on the 15 L bioreactor to optimize the controller tuning parameters. Process-model mismatch was avoided in the simulation control charts (Fig. 4d–f). A prediction horizon ( $P$ ) and a control horizon ( $M$ ) of 1 were chosen due to the large sample interval and values of zero were utilized for the diagonal elements of the input ( $\Lambda$ ) and output ( $\Gamma$ ) weight matrices. The measurement infrequency (lack of noise) and the SISO nature of the control loop justified the use of these weights. Finally, input magnitude constraints of  $0 \text{ L h}^{-1} \leq u \leq 4.07 \times 10^{-2} \text{ L h}^{-1}$  were imposed on the feed rate ( $u$ ). No constraints were set on the process variable. It was observed from Fig. 4 that the simulated and real-time NMPCs produced COs with similar trends and based on the NMPCs prediction capabilities, feeding initiated at 36 h in both instances to avoid the PV dropping below the set-point before the next control point at 48 h. Incorporation of the longer controller sample time of 12 h highlights one of the true benefits of the NMPC to be able to predict into the future and optimize the controller action for a bioprocess system, which traditionally is sub-optimal based on bolus feeds calculated from offline measurements or open loop predefined feeding strategies. Classical PID control would not initiate the control action until the PV is below the set-point which can be detrimental to controller performance when operating with long sample times which are common in bioprocessing. In order to prevent the negative

effect of erroneous readings from the Raman probe such as saturated spectra, the PV was time averaged over 30 min to ensure a representative reading for the NMPC.

Fig. 5 illustrates the process model performance for the glucose concentration in real-time in comparison to the on-line Raman readings and the off-line calculations. The applicability of the Raman calibration model is justified as it provides a clear representation of the real environment (Fig. 5). However, it is evident that mismatch occurred between the on-line plant readings and the model predictions throughout the 15 L NMPC run. This was due to the natural variability in biological systems. Boudreau and McMillan [2] stated that a typical bioprocess plant's coefficient of variation (CV) is approximately 10%, which is significantly higher than that for small molecule chemical processes for pharmaceuticals.

Measurement errors are inherent with both the on-line and off-line glucose measurement methods. The off-line estimation of the glucose concentration by the Nova Bioprofile 400 has a typical measurement error of 4% which should be considered when analyzing the off-line data [41]. Similarly, the standard error of prediction (SEP) of the on-line Raman PLS calibration model is 1.82 mM [32].

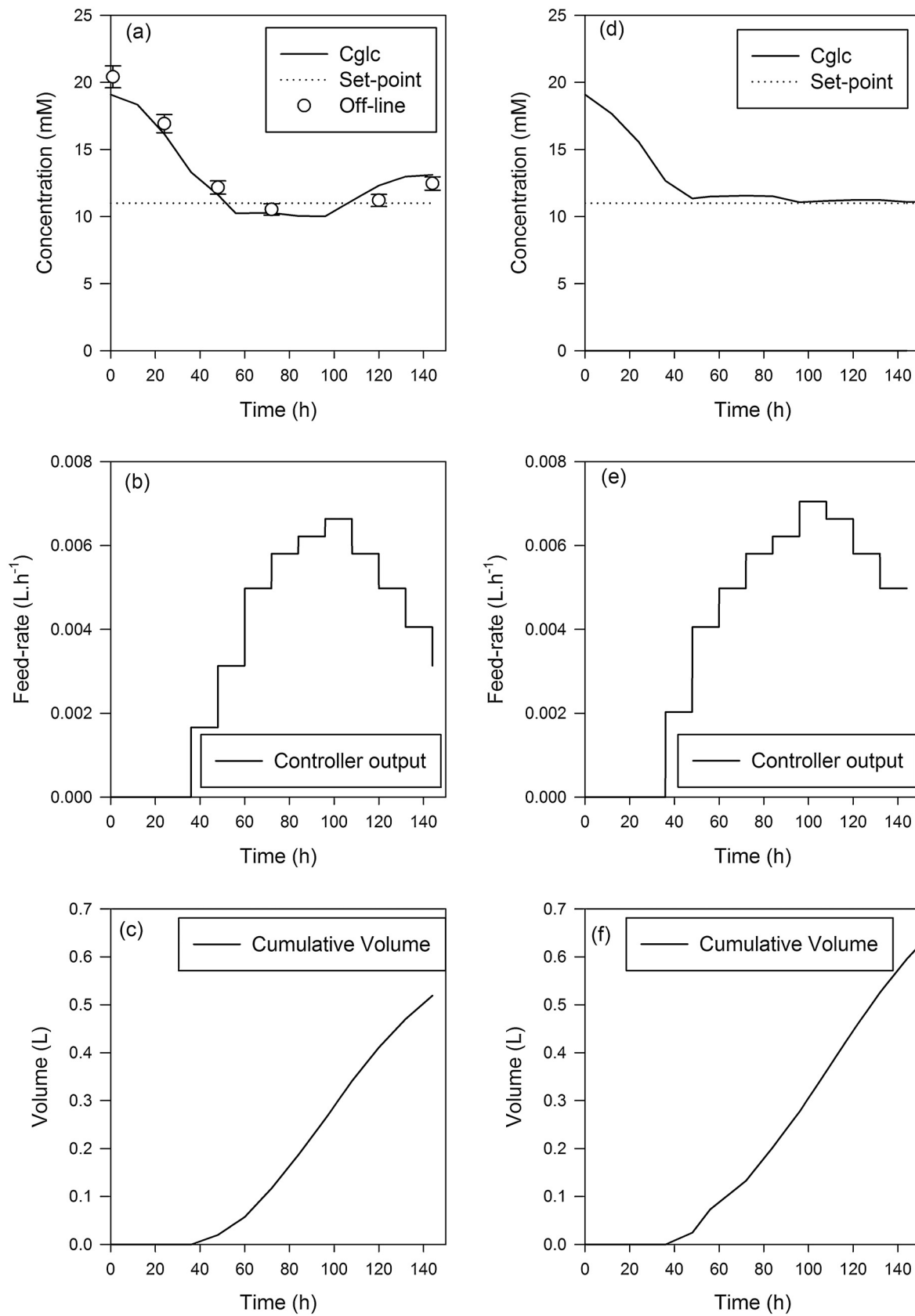
The initial offset between the process readings and the model is due to the absence of a cell density lag phase (0–24 h) in the process model and thus the cell number in the bioreactor increases at a faster rate, earlier than expected and therefore leads to a higher predicted glucose consumption rate. Discrepancies between the process model and the plant readings were also evident toward the end of the batch when the glucose concentrations from the process model fell in response to the lower feed-rates from the NMPC. This indicates that the model was over-predicting the rate of glucose consumption (Fig. 5) as a result of an under-prediction in the rate of cell death toward the end of the batch (Fig. 6a). As a result of this mismatch present, the controller slightly under-performed (Fig. 4a) compared to the simulated control chart with zero mismatch (Fig. 4d). Table 3 quantifies the simulated and real-time NMPC performances. As would be expected the idealized zero mismatch simulated NMPC had lower performance indices. The ITAE value for the real plant was higher due to the PV under and overshooting for to a greater magnitude for a longer period of time. However, the real-time NMPC performance resulted in ISE and IAE values very close to that of the optimal simulated NMPC, highlighting the success of the real-time NMPC.

Fig. 6 presents the real-time model predictions and off-line data for the viable cell density, substrates and metabolites. The on-line Raman readings were also shown for the glutamine, lactate and ammonia concentrations. The results in Fig. 6 illustrate an over-prediction in the glutamine concentration by the Raman PLS calibration model for the first half of the batch and an under-prediction in the ammonia concentration for the second half of

**Table 3**  
NMPC performance indices with a 12 h measurement interval.

Index	Simulation NMPC ( $P=1, M=1, \Gamma=1, \Lambda=0$ )	Real NMPC ( $P=1, M=1, \Gamma=1, \Lambda=0$ )
ISE	134	165
ITAE	476	1336
IAE	24	33





**Fig. 4.** NMPC fixed set-point tracking performance for (a = real, d = simulated) glucose, (b = real, e = simulated) the corresponding controller output and (c = real, f = simulated) cumulative feed volumes for a 15 L fed-batch bioprocess with a 12 h measurement interval. Error bars represent the standard deviation of the off-line reference method.

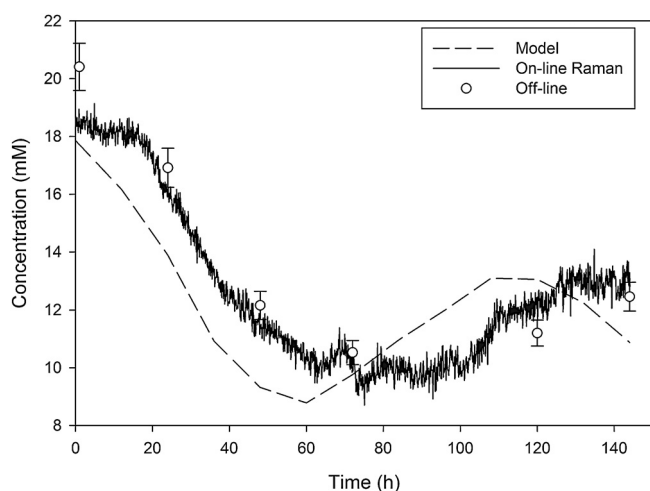


Fig. 5. 15 L NMPC (12 h) glucose concentration process model, off-line data and on-line Raman measurements. Error bars represent the standard deviation of the off-line reference method.

the batch. An iC Raman auto-calibration also occurred at 72 h into the batch which had a noticeable effect on the Raman outputs (Fig. 6).

Overall, the off-line data compared well to the process model predictions for all substrates and metabolites apart from lactate. The off-set between the lactate off-line data and the model predictions was a function of the lactate model being initialized with non-representative on-line lactate Raman readings.

With the availability of more experimental data, the process model can be further refined to better represent the process to be controlled and improve NMPC performance for closed loop fixed set-point tracking of the glucose concentration within the bioreactor.

NMPC proved to be successful for this 140 h fed-batch bioprocess which illustrated the long measurement intervals, changing process dynamics and inherent process variation associated with biological systems. With the availability of an appropriate bioprocess model, this advanced control strategy eliminated the labor intensive nature of manual control prevalent in the bioprocess industry.

### 3.3. Process-model mismatch, process disturbances and measurement noise

Real-time NMPC applications will inevitably experience plant-model mismatch. It is nearly impossible to create the perfect bioprocess model especially due to their inherent variability. In an attempt to analyze NMPC performance in the presence of process-model mismatch, the bioprocess model parameters relating to nutrient consumption were deliberately altered to cause mismatch in the process model glucose consumption (Table 4). The controller sampling interval was reduced from 12 h to 0.1 h to aid the feedback correction in the presence of process-model mismatch. Measurement noise from the on-line Raman readings was prominent due to this increase in measurement frequency.

The controller was re-tuned in order to obtain a robust real-time NMPC with good performance capabilities in the presence of mismatch and measurement noise. From an implementation standpoint, the prediction horizon ( $P$ ) and the control horizon ( $M$ ) were not practical to use as tuning parameters.  $P$  and  $M$  were chosen as 40 and 2 respectively. The control horizon of 2 was chosen because it is known that increasing  $M$  can stabilize an

Table 4  
Sub-optimal model parameters.

Parameter	Unit	Value
$k_{d,Q}^a$	$\text{h}^{-1}$	0.001
$m_G^a$	$\text{mmol cell}^{-1} \text{h}^{-1}$	$8.0 \times 10^{-13}$
$Y_{A,Q}^b$	–	1.10
$Y_{L,G}^b$	–	4.0
$Y_{X,G}^b$	$\text{cells mmol}^{-1}$	$1.50 \times 10^8$
$Y_{X,Q}^b$	$\text{cells mmol}^{-1}$	$1.9 \times 10^9$
$K_L^a$	mM	150
$K_A^a$	mM	40
$k_{d,\max}^b$	$\text{h}^{-1}$	0.01
$\mu_{\max}^b$	$\text{h}^{-1}$	0.048
$K_G^a$	mM	1.0
$K_Q^a$	mM	0.22
$m_Q^a$	$\text{mmol cell}^{-1} \text{h}^{-1}$	0
$k(\mu)^a$	$\text{h}^{-1}$	0.01
$K_{\text{LYSIS}}^a$	$\text{h}^{-1}$	0
$C_i^a$	mM	100
$q_i^a$	$\text{mmol cell}^{-1} \text{h}^{-1}$	$3.5 \times 10^{-10}$

<sup>a</sup> Fitted model parameter.

<sup>b</sup> Experimentally determined model parameter.

NMPC system in the presence of process-model mismatch. It is also known from robustness analysis studies using perturbation theory that increasing  $M$  increases the controller performance [42]. However, increasing the control horizon leads to increased computational load. Therefore, a balance needs to be met between controller robustness, performance and computational load. The time required to solve the NMPC optimization algorithm was approximately 2 min. However, there were no convergence issues due to the sample time being longer (6 min). The diagonal elements of the output weight matrix ( $\Gamma$ ) were set at 1 due to the ‘single input – single output’ (SISO) nature of the NMPC. The diagonal elements of the input weight matrix ( $\Lambda$ ) were set a value of 60 to help limit erratic control action movements in response to measurement noise. Finally, the feed-rate was constrained as before and no output magnitude constraints were imposed for the glucose concentration. Fig. 7 presents the real-time and corresponding simulation control results for the NMPC ( $P=40$ ,  $M=2$ ,  $\Lambda=60$ ,  $\Gamma=1$ ) 15 L pilot scale fed-batch bioprocess. The NMPC performance was simulated with zero process-model mismatch.

The NMPC closed loop fixed set-point tracking on the 15 L bioreactor was initially hampered with the occurrence of non-modeled pump operational difficulties between 35 and 45 h and between 58 and 60 h (Fig. 7a). This was caused by a blockage in the feed bottle vent line which prevented the pump delivering the calculated feed volumes. Therefore, the on-line Raman glucose concentration readings dropped despite the NMPC calculating increased feed-rates (Fig. 7b) to combat the observed undershoots. This issue was resolved by replacing the filter on the vent line of the feed bottle. Such operational difficulties were not considered in the building of the process model.

The 15 L process model was built with a sub-optimal parameter set. As a result, the NMPC in real-time delivered higher flow-rates (Fig. 7b) than those depicted in simulation mode (Fig. 7e) and thus augmented the mismatch (Fig. 8). It also has to be noted that bioprocesses present an inherent variability which can affect model applicability [2]. Due to the deliberate presence of process-model mismatch, it was not possible to successfully use the NMPC capabilities to both dampen out the control action and result in an adequate system response.

In summary, the unavailability of a representative process model and non-modeled disturbances encountered during the real-time implementation of NMPC contributed to the presence of process-model mismatch (Fig. 8). The mismatch present led to a

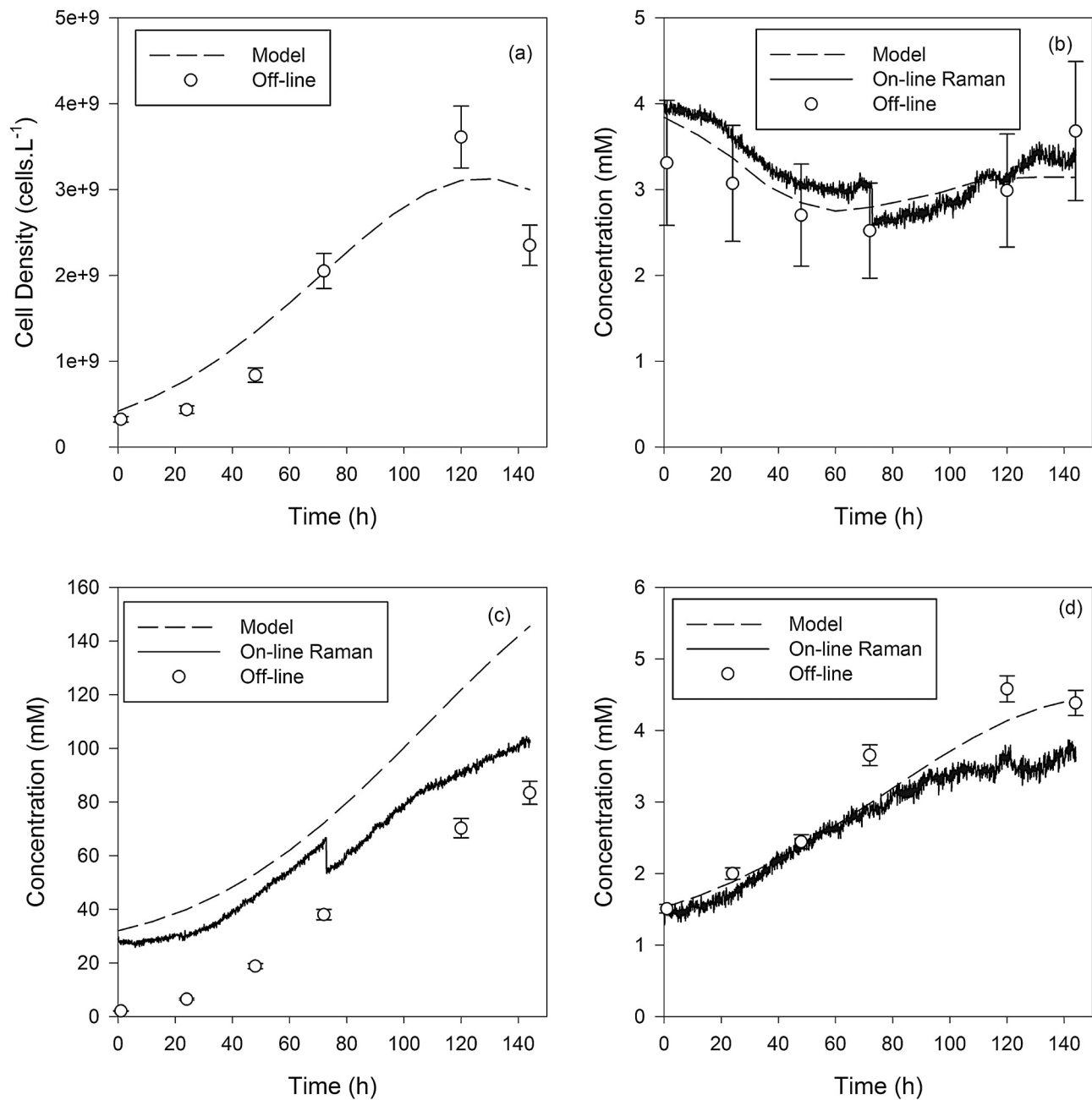


**Fig. 6.** 15 L NMPC (12 h) real-time (a) viable cell density, (b) glutamine, (c) lactate and (d) ammonia model. Error bars represent the standard deviation of the off-line reference method.

consistent undershoot of approximately 1 mM from the defined set-point (Fig. 7a). However, this result would be acceptable for bioprocess nutrient concentration control. However, when operating under longer sample intervals performance degradation would increase due to the infrequency of the feed-back corrective action. The simulated and real-time controller performances are quantified in Table 5. The ISE and IAE values were larger for the simulated NMPC due to the fact the modeled glucose consumption rate differed from the real process and as a result it took slightly longer for the PV to initially reach the defined set-point of 11 mM (Fig. 7b). However the ITAE is a more appropriate measure of controller performance. Non-modeled disturbances and sub-optimal model performance led to a higher ITAE in the real environment.

Process-model mismatch is inevitable but all efforts should be taken to ensure its presence is minimized by building robust process models and ensuring real-time plant data is accurate and representative of the true behavior of the plant.

**Table 5**  
NMPC performance indices with a 0.1 h measurement interval and mismatch.

Index	Simulation NMPC ( $P=40$ , $M=2$ , $\Gamma=1$ , $\Delta=60$ )	Real NMPC ( $P=40$ , $M=2$ , $\Gamma=1$ , $\Delta=60$ )
ISE	10,072	7839
ITAE	72,206	89,963
IAE	2312	2253

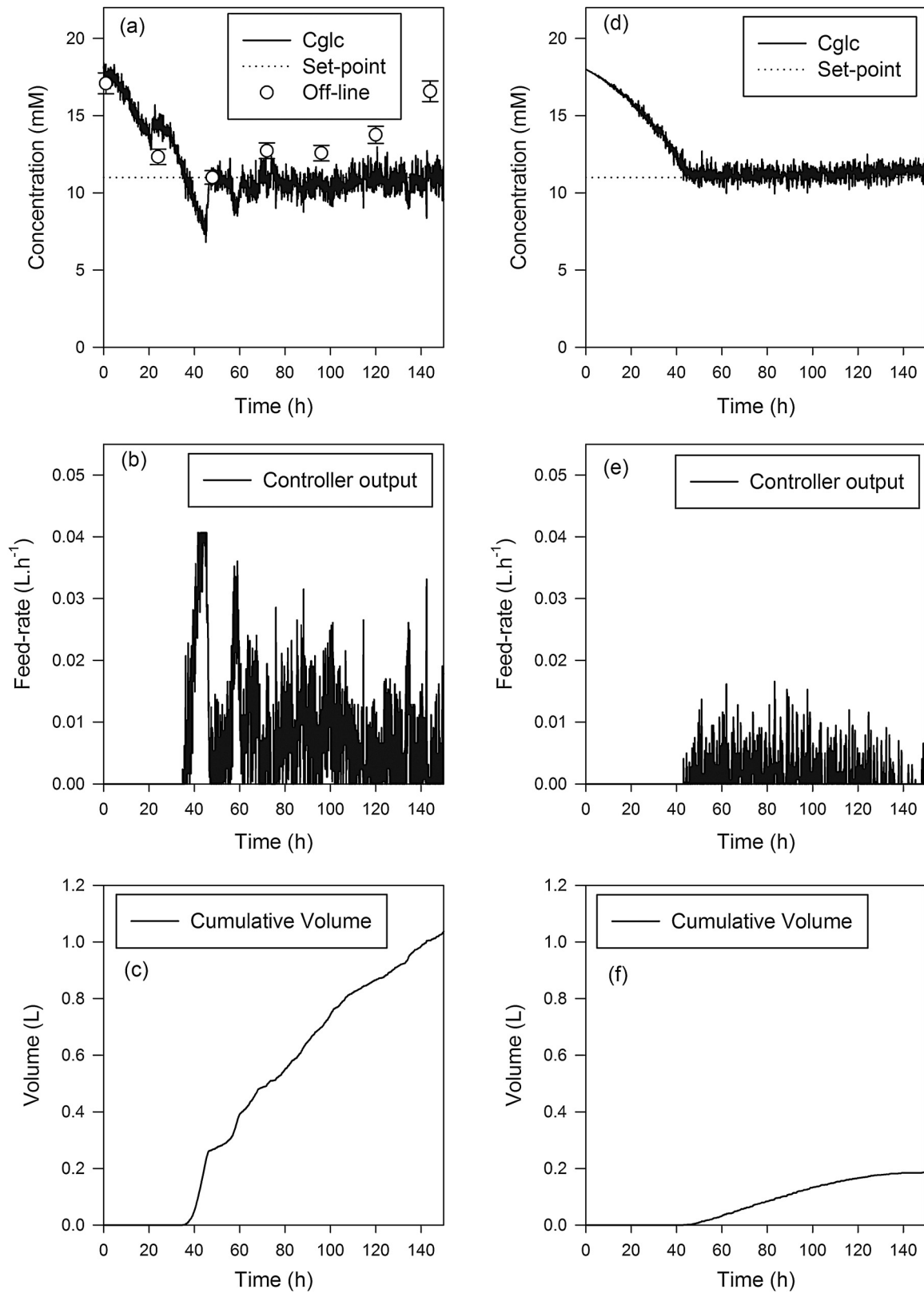


**Fig. 7.** NMPC fixed set-point tracking performance with process-model mismatch for (a = real, d = simulated) glucose, (b = real, e = simulated) the corresponding controller output and (c = real, f = simulated) cumulative feed volumes for a 15 L fed-batch bioprocess with a 0.1 h measurement interval. Error bars represent the standard deviation of the off-line reference method.

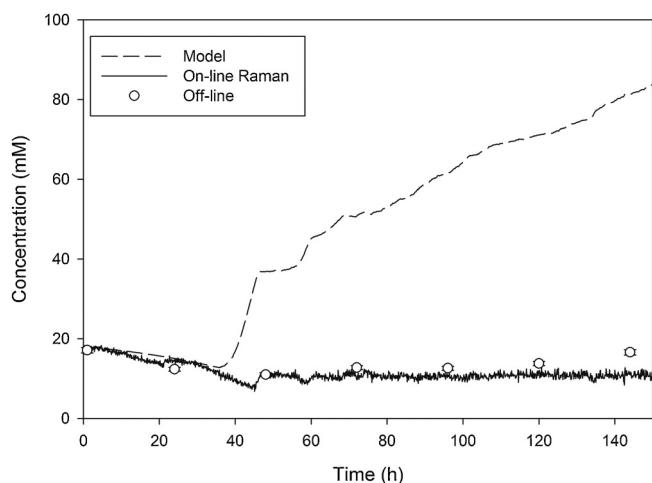


Fig. 8. 15 L NMPC (0.1 h) glucose concentration process model, off-line data and on-line Raman measurements. Error bars represent the standard deviation of the off-line reference method.

#### 4. Conclusions

Process control of bioprocesses presents significant problems in comparison to small molecule chemical processes for pharmaceuticals. Nonlinear model predictive control (NMPC) was successful in controlling the bioprocess environment with associated negative attributes such as high process variability, measurement noise and long measurement intervals. The bioprocess was equipped with an on-line Raman spectroscopic probe. Utilization of such PAT techniques leads to an increase in the measurement frequency of the CPPs which are traditionally measured infrequently at- or off-line in the biopharmaceutical industry.

Offline simulation studies of controller performance before real-time application provided a platform to understand and potentially optimally tune a NMPC to avoid the difficulties associated in controlling a bioprocess environment.

The main real-time implementation difficulties experienced with NMPC was process-model mismatch. The unavailability of representative experimental data to build a robust valid process model can have major implications for NMPC performance. The high variability associated with bioprocesses also leads to an augmentation of this problem. In a bioprocess environment where long measurement times are prevalent; more emphasis is applied to the NMPC prediction capabilities. In the presence of long controller measurement intervals, and the availability of an appropriate process model, NMPC provided satisfactory controller performance. Therefore, NMPC with the availability of an appropriate bioprocess model has the potential to allow the biopharmaceutical industry to optimize their bioreactor feeding strategies based on the norm of infrequent at-line process variable measurements.

In a PAT driven process, where a spectroscopic probe is used to monitor important process variables online frequently, model applicability is less of an issue to controller performance. However, spectroscopic techniques such as Raman and mid IR are associated with high measurement noise. The NMPC controller was successfully tuned in an off-line simulator to deal with this operation issue. However, in real-time due to the presence of process-model mismatch, measurement noise dampening had to be balanced with controller set-point tracking performance.

After careful consideration and attempted mitigation of the problems associated with the bioprocess control, closed loop NMPC fixed set-point tracking of the nutrient concentration in a 15 L pilot scale bioreactor was accomplished even in the presence of

process-model mismatch, process disturbances, high measurement noise and long process variable measurement intervals. In conclusion, NMPC is a promising technology for the optimal control of bioprocesses.

#### Acknowledgement

This work was carried out as part of the 'Bio Application of PAT (apPAT)' project, an Enterprise Ireland funded Industry Led Research Project.

#### References

- [1] G. Walsh, Biopharmaceutical benchmarks 2010, *Nat. Biotechnol.* 28 (9) (2010) 917–924.
- [2] M. Boudreau, G. McMillan, New Directions in Bioprocess Modeling and Control: Maximising Process Analytical Technology Benefits, ISA, Research Triangle Park, NC, 2006.
- [3] A. Gambhir, Alteration of cellular metabolism by consecutive fed-batch cultures of mammalian cells, *J. Biosci. Bioeng.* 87 (1999) 805–810.
- [4] K. Wlaschin, W.-S. Hu, Fedbatch culture and dynamic nutrient feeding, *Adv. Biochem. Eng. Biotechnol.* 101 (2006) 43–74.
- [5] L. Xie, D.I. Wang, Fed-batch cultivation of animal cells using different medium design concepts and feeding strategies, *Biotechnol. Bioeng.* 43 (11) (1994) 1175–1189.
- [6] L. Xie, D.I. Wang, Applications of improved stoichiometric model in medium design and fed-batch cultivation of animal cells in bioreactor, *Cytotechnology* 15 (1994) 17–29.
- [7] J.A. Lopes, P.F. Costa, T.P. Alves, J.C. Menezes, Chemometrics in bioprocess engineering: process analytical technology (PAT) applications, *Chemometr. Intell. Lab. 74* (2) (2004) 269–275.
- [8] F. Lu, P. Choo Toh, I. Burmet, F. Li, T. Hudson, A. Amanullah, J. Li, Automated dynamic fed-batch process and media optimization for high productivity cell culture process development, *Biotechnol. Bioeng.* 110 (1) (2013) 191–205.
- [9] Y. Lee, Low-glutamine fed-batch cultures of 293-HEK serum-free suspension cells for adenovirus production, *Biotechnol. Prog.* 19 (2003) 501–509.
- [10] L. Li, Increasing the culture efficiency of hybridoma cells by the use of integrated metabolic control of glucose and glutamine at low levels, *Biotechnol. Appl. Biochem.* 42 (2005) 73–80.
- [11] J.H. Lee, B. Cooley, Recent advances in model predictive control, in: *Chemical Process Control-V*, vol. 93 (316), *AIChE Symposium Series – American Institute of Chemical Engineers*, 1997, pp. 201–216.
- [12] S.J. Qin, T.A. Badgwell, An overview of industrial model predictive control technology, in: *Chemical Process Control-V*, vol. 93 (316), *AIChE Symposium Series – American Institute of Chemical Engineers*, 1997, pp. 232–256.
- [13] W.H. Kwan, S.H. Han, *Receding Horizon Control: Model Predictive Control for State Models*, Advanced Textbooks in Control and Signal Processing Series, Springer, London, 2005.
- [14] J.A. Rossiter, *Model-Based Predictive Control: A Practical Approach*, CRC Press, New York, 2003.
- [15] J.B. Rawlings, D.Q. Mayne, *Model Predictive Control: Theory and Design*, Nob Hill Publishing, Madison, Wisconsin, 2009.
- [16] S.J. Qin, T.A. Badgwell, A survey of industrial model predictive control technology, *Control Eng. Pract.* 11 (7) (2003) 733–764.
- [17] M. Aehle, K. Bork, S. Schaepe, A. Kuprijanov, R. Horstkorte, R. Simutis, A. Lubbert, Increasing batch-to-batch reproducibility of CHO cultures using a model predictive control approach, *Cytotechnology* 64 (2012) 623–624.
- [18] A. Ashoori, B. Moshiri, A. Khaki-Sedigh, M.R. Bakhtiari, Optimal control of a nonlinear fed-batch fermentation process using model predictive approach, *J. Process Contr.* 19 (2009) 1162–1173.
- [19] S.J. Qin, T.A. Badgwell, An overview of nonlinear model predictive control applications, in: J.C. Kantor, C.E. Garcia, B. Carnahan (Eds.), *Nonlinear Model Predictive Control*, Birkhauser, Basel, 2000.
- [20] R. Findeison, F. Allgower, L. Biegler, *Assessment and Future Directions of Nonlinear Model Predictive Control*, Springer-Verlag, Berlin/Heidelberg, 2007.
- [21] M. Lawrynczuk, Modelling and nonlinear predictive control of a yeast fermentation biochemical reactor using neural networks, *Chem. Eng. J.* 145 (2) (2008) 290–307.
- [22] D. Şendrescu, Nonlinear model predictive control of a depollution bioprocess, in: *Proc. of the 3rd Pacific-Asia Conference on Circuits, Communications and System (PACCS'11)*, vol. 1 (1–4), Wuhan, China, 2011.
- [23] Z.K. Nagy, Model based control of a yeast fermentation bioreactor using optimally designed artificial neural networks, *Chem. Eng. J.* 127 (1–3) (2007) 95–109.
- [24] F. Allgöwer, A. Zheng, *Nonlinear Model Predictive Control. Progress in System and Control Theory*, vol. 26, Birkhäuser Verlag, 2000.
- [25] F. Eduardo, C. Bordons, *Model Predictive Control, Advanced Textbooks in Control and Signal Processing*, 2nd ed., Springer, London, 2004.
- [26] L. Grune, J. Pannek, *Nonlinear Model Predictive Control. Theory and Algorithms*, 1st ed., Springer-Verlag, London, 2011.



- [27] L. Magni, D.M. Raimondo, F. Allgower, Nonlinear Model Predictive Control. Towards New Challenging Applications, Lecture Notes in Control and Information Sciences, vol. 384, Springer-Verlag, Berlin/Heidelberg, 2009.
- [28] B. Kouvaritakis, M. Cannon, Nonlinear Model Predictive Control: Theory and Practice, vol. 61, Institution of Electrical Engineers, 2001.
- [29] B.W. Bequette, Non-linear model predictive control: a personal retrospective, *Can. J. Chem. Eng.* 85 (4) (2007) 408–415.
- [30] M.J. Tenny, J.B. Rawlings, S.J. Wright, Closed loop behaviour of nonlinear model predictive control, *AIChE J.* 50 (9) (2004) 2142–2154.
- [31] Z. Nagy, R. Findeisen, M. Diehl, F. Allgower, H.G. Bock, S. Agachi, J.P. Schlöder, D. Leineweber, Real-time feasibility of nonlinear predictive control for large scale processes—a case study, in: *Proc. of ACC, Chicago, IL, 2000*.
- [32] J. Whelan, S. Craven, B. Glennon, In-situ Raman spectroscopy for simultaneous monitoring of multiple process parameters in mammalian cell culture bioreactors, *Biotechnol. Progr.* 28 (5) (2012) 1355–1362.
- [33] M. Buehren, Matlab Central File Exchange. February 3, 2008, Available at <http://www.mathworks.com/matlabcentral/fileexchange/18593-differential-evolution>
- [34] S. Craven, N. Shirsat, J. Whelan, B. Glennon, Modeling a mammalian cell bioprocess for different operation modes and bioreactor scales, *Biotechnol. Progr.* 29 (1) (2013) 186–196.
- [35] C.R. Cutler, B.L. Ramaker, Dynamic matrix control—a computer control algorithm, in: *Proc. of the Joint Automatic Control Conference*, 1980.
- [36] P.T. Boggs, J.W. Tolle, Sequential quadratic programming for large scale nonlinear optimization, *J. Comput. Appl. Math.* 124 (2000) 123–137.
- [37] L.T. Biegler, I.E. Grossmann, A.W. Westerberg, Systematic Methods of Chemical Process Design, Prentice Hall, Upper Saddle River, NJ, 1997.
- [38] M. Diehl, R. Findeisen, S. Schwarzkopf, I. Uslu, F. Allgower, H.G. Bock, E.D. Gilles, J.P. Schlöder, An efficient algorithm for nonlinear model predictive control of large-scale systems. Part 1: Description of the method, *Automatisierungstechnik* 50 (12) (2002) 557–567.
- [39] E. Zafriou, A. Marchal, Stability of SISO quadratic dynamic matrix control with hard output constraints, *AIChE J.* 37 (1991) 1550–1560.
- [40] D. Nagrath, V. Prasad, B.W. Bequette, Model Predictive Control of Open-Loop Unstable Cascade Systems, *American Control Conference*, Chicago, IL, 2000.
- [41] N.R. Abu-Absi, B.M. Kenty, M.E. Cuellar, M.C. Borys, S. Sakhamuri, D.J. Strachan, M.C. Hausladen, Z.J. Li, Real-time monitoring of multiple parameters in mammalian cell culture bioreactors using an in-line Raman spectroscopy probe, *Biotechnol. Bioeng.* 108 (5) (2001) 1215–1221.
- [42] K.Z. Qi, D.G. Fisher, Robust stability of model predictive control, in: *Proc. of the American Control Conference*, Baltimore, MD, 1994, pp. 3258–3262.